Query Details

Back to Main Page

1. Please confirm if the author names are presented accurately and in the correct sequence (given name, family name). Author 8 Given name: [Maria Perla] Last name [Colombini], Author 9 Given name: [Maria Rosaria] Last name [Tinè]. Also, kindly confirm the details in the metadata are correct.

The author names are correct including Authors 8 and 9

2. Please check and confirm the organization name is correctly identified for the affiliation 2.

The organization name (affiliation2) is correct

3. Please check the edit made in the article title.

the edit is ok

4. Please check whether the edit made in the sentence 'Results obtained are summarized … composition of the different pigments' conveys the intended meaning.

The edit is correct

5. Please provide complete details for the references [3, 4, 5].

3. Colombo L. I colori degli antichi, Ed. Nardini, 1995 ISBN-10: 8840440356, ISBN-13: 978-8840440354
4. Barrie B.. Artist's pigments: a handbook of their history and characteristics,Archetipe Publications, London (UK),Vol. 4, 2007
5. Mayer R. The artist's handbook of materials and techniques,Third Edition, The Viking press, New York, 1970.SBN 670-13665-4

6. Please check and confirm the inserted article title is correct for the reference [43].

The title is correct

7. Please provide publication year for the references [51, 52].

51 Dohnalová, Ž., Šulcová, P. & Bělina, P. J Therm Anal Calorim (2019). https://doi.org/10.1007/s10973-019-08522-z
52Dohnalová, Ž., Šulcová, P. & Bělina, P. J Therm Anal Calorim (2019). https://doi.org/10.1007/s10973-019-08522-z

8. References [64, 65] are given in the list but not cited in text. Please cite in text or delete from the list.

Now all the references are cited in the text

A multi-analytical characterization of artists' carbon-based black pigments

Anna Lluveras-Tenorio, [1]

Alessio Spepi, [1]

Matteo Pieraccioni, [1]

Stefano Legnaioli, [2]

Giulia Lorenzetti, [2]

Vincenzo Palleschi, [2]

Marius Vendrell, [3]

Maria Perla Colombini, [1]

Maria Rosaria Tinè, [1]

Celia Duce, [1]✉

Email celia.duce@unipi.it

Ilaria Bonaduce, [1]

[1] Department of Chemistry and Industrial Chemistry, University of Pisa, Via G. Moruzzi 13, 56124 Pisa, Italy

[2] National Research Council of Italy, C.N.R., Institute of Chemistry of Organo Metallic Compounds-ICCOM-UOS Pisa, Via G. Moruzzi 1, 56124 Pisa, Italy

[3] Departament de Cristal.lografia, Mineralogia i Dipòsits Minerals, Universitat de Barcelona, Carrer Marti i Franquès s/n, 08028 Barcelona, Spain

Received: 6 May 2019 / Accepted: 10 October 2019

Abstract

The most common synthetic carbon-based black pigments can be divided into three main groups on the basis of the material used for their production: bone blacks, vine blacks and lampblacks. This work reports on the physicochemical

characterization of the three commercial pigments purchased from Kremer Pigmente (Germany) and Zecchi (Italy) by means of a multi-analytical approach, which included thermoanalytical (thermogravimetry, thermogravimetry coupled with FTIR and differential scanning calorimetry) and spectroscopic techniques (laser-induced breakdown spectroscopy, Fourier-transform infrared spectroscopy, Raman spectroscopy and X-ray powder diffraction). Combining the results obtained from this multi-analytical approach, qualitative and quantitative conclusions are drawn for the first time. Lampblacks are mainly composed of amorphous carbon. In vine black (Kremer), amorphous carbon and cellulose pyrolysis by-products are the main constituents. In bone blacks and vine black (Zecchi), carbonaceous materials are minor components. Hydroxyapatite and calcium carbonate are the main constituents of bone blacks, and iron and magnesium oxides are the main constituents of vine black (Zecchi). Results from this multi-analytical study on the composition of such widespread pigments can provide valuable information in the decision-making process for restorers and conservators.

AQ1

AQ2

Keywords

Black pigments
Thermogravimetry
Differential scanning calorimetry
Raman spectroscopy
FTIR analysis
LIBS

Electronic supplementary material

The online version of this article (https://doi.org/10.1007/s10973-019-08910-5) contains supplementary material, which is available to authorized users.

Anna Lluveras-Tenorio and Alessio Spepi have contributed equally to this work.

Introduction

Pigment identification is key to understanding the history of an artwork, the technical know-how of a culture, trade routes and the solution of problems related to conservation, restoration, dating and artist attribution. Pigments have been used for the authentication of Russian Icons [1] or to establish that the trading of Indian lac was already occurring back in the twelfth century [2].

AQ3

Black pigments are synthetic pigments that can be found in paintings, polychromies and archeological artifacts [3, 4, 5]. They have a long history, being the first pigments to be used in prehistory identified in archeological painted plaquettes from Paleolithic caves in Spain [6], in the prehistoric wall paintings from Domus Janas necropolis (Italy) [7] or in the ink residues from a Qumran inkwell [8]. Carbon-based pigments form a very diverse group which includes many subgroups, such as crystalline carbon, flame carbons, chars, cokes and black hearts. However, in art, they are generally identified by the source or manufacturing process used in their production. [9, 10, 11, 12, 13, 14, 15, 16, 17, 18, 19, 20].

Carbon black was the first black used. This dull black is the easiest to manufacture as it is made of charcoal. Vine black, traditionally made by charring desiccated grape vines and stems, is a beautiful bluish black. Bone black, synthesisted since prehistoric times by burning bones, is the darkest black available. Lampblack, the most recent pigment of the group, was traditionally manufactured by collecting soot from oil lamps. Many techniques have been used for identifying black pigments in artworks, including SEM–EDS [9, 13, 16, 21], laser-induced breakdown spectroscopy (LIBS) [22, 23, 24, 25, 26], Fourier-transform infrared spectroscopy (FTIR) [13, 16, 27, 28, 29, 30, 31, 32, 33, 34] and Raman spectroscopy [11, 13, 16, 35, 36, 37, 38, 39, 40].

However, identifying carbon-based pigments in paintings and polychromies is not straightforward. The absence of any element (such as Mn or Fe) or crystallographic pattern associated with other black pigments, such as magnetite (Fe_3O_4) or pyrolusite (MnO_2) [18, 19], is considered as an evidence of the use of a carbon-based black [20]. Raman seems to be the best nondestructive technique to establish the presence of black carbon pigments in artworks [35, 37, 40, 41, 42]. The noninvasive in situ nature of Raman analysis has been key in the identification of carbon black pigments in prehistoric mural paintings from the Paleolithic rock art of Quercy (France) [43]. The presence of P from the elemental analysis and the observation of the band at ca 961 cm^{-1} in the Raman spectrum typical of PO_4^{3-} are used as an indicator of bone/ivory black [21].

Reference materials, mainly lampblack, wine, bone and ivory black together with bitumen, Mars black, Van Dick black all from Zecchi Colori Belle Arti (Italy) and Kremer Pigmente (Germany), have been investigated in the literature by means of different techniques such as FTIR and Raman in order to establish criteria to distinguish the origin of various carbon black pigments [11, 27, 28, 34].

When studied by Raman, synthetic carbon-based pigments present similar spectral features (two broad and overlapping bands centered at 1580 and 1350 cm^{-1}) [11, 27]. However, the statistical combined analysis of spectral parameters enabled pigment differentiation [27]. In another study, ten synthetic carbon-based black pigments were characterized by a combination of FTIR-ATR, Raman, SEM–EDS and XRD to establish discriminative criteria [37]. However, the results mainly highlighted that little is known about the pigment actual compositions and that the information described on the labels is misrepresenting.

Thermoanalytical techniques have recently been applied in the field of cultural heritage to characterize organic and inorganic pigments, in particular to study their nature, thermal stability and interactions with binders [41, 42, 44, 45, 46, 47, 48, 49, 50, 51, 52]. Thermogravimetry in air of powdered reference black pigments purchased from specialized producers has been reported in the work of Gatta et al. [53]. Data were used to identify the black pigment in an ancient Roman wall painting (Imperial Age, 30 B.C.).

In this work, the three among the most commonly used synthetic carbon-based black pigments (bone black, vine black and lampblack, purchased from two different specialized manufacturers—Zecchi and Kremer) were studied and compared using a multi-analytical approach. Raman spectroscopy was used to discriminate between crystalline and amorphous carbon structures. LIBS characterized the elemental content, and when used with XRD it revealed traces of inorganic species. FTIR gave information mostly on the organic parts of the pigments. Thermoanalytical analysis enabled us to study the thermal stability of the pigments, their decomposition products and their inorganic/organic ratio. To the best of our knowledge, differential scanning calorimetry (DSC) and thermogravimetry coupled with FTIR for evolved gas analysis (TG-FTIR) under nitrogen flow have not been performed on black pigments to date. The aim of this study was to provide detailed information on the chemical composition, thermal stability and physicochemical characteristics of the investigated pigments, highlighting qualitative and quantitative differences. Results from this multi-analytical study on the composition of such widespread pigments provide valuable information in the decision-making process for restorers and conservators.

Experimental

Materials

The reference materials used for this study were bone black, vine black and lampblack purchased from Kremer Pigmente (Germany) and Zecchi (Italy). The commercial names and reference numbers are specified in Table 1.

Table 1

Reference black pigments studied: commercial name, manufacturer, source of pigment as described by the manufacturer

Commercial name and catalog number	Source of pigment as described by the manufacturer	Manufacturer
Ivory Black-0979	Charred ivory–calcium phosphate containing carbon	Zecchi
Bone Black-47100	Carbonization of bones over 400C	Kremer
Vine Black-0941	Vegetal carbon	Zecchi
Vine Black-4700	Carbon, insoluble carbon compounds and ashes	Kremer
Lampblack-C0998	Residue of carbonization	Zecchi
Lampblack-47250	Nearly pure amorphous carbon	Kremer

The reference materials were studied as it is. The lampblack samples were pre-dried before DSC analysis and TG analysis under oxygen.

Methods

A summary of the techniques employed in this work starting with the nondestructive and leading to the destructive ones is reported in Scheme 1.

Scheme 1

Flowchart of the techniques employed in this work from the nondestructive to the destructive ones

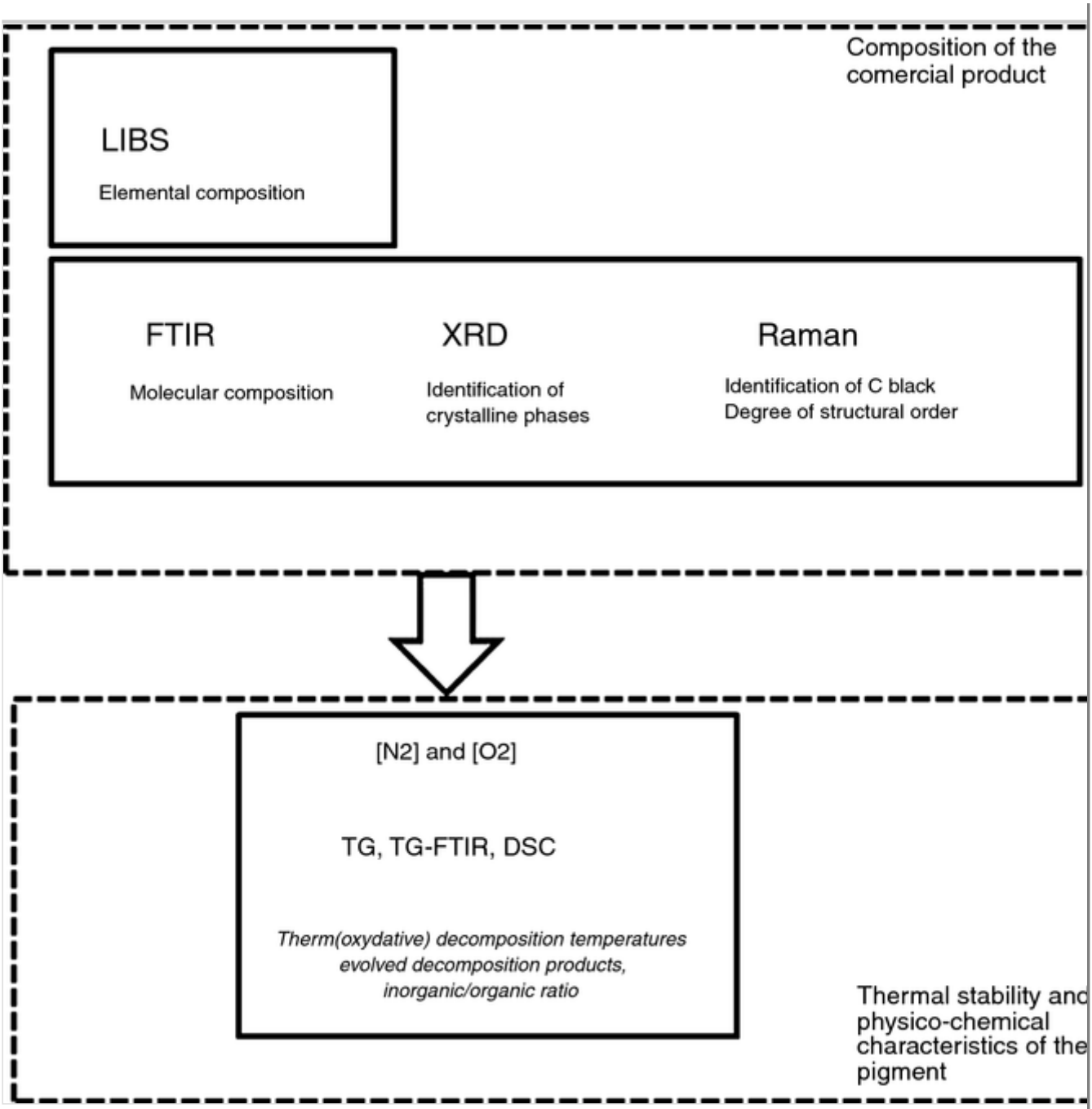

A TA Instruments Thermobalance model Q5000IR was used. Measurements were performed at a rate of 10 °C min^{-1}, from 30 to 1000 °C under nitrogen and 800 °C under airflow (25 ml min^{-1}). The amount of sample in each TG measurement varied between 2 and 4 mg. TG balance was calibrated for the weight by means of weighted platinum calibrated pans. The temperature calibration was performed measuring the Curie point of a set of three magnetic standards. The same instrument equipped with an FTIR Agilent Technologies spectrophotometer model Cary 640 for evolved gas analysis (EGA) was used for the TG-FTIR experiments. TG-FTIR measurements were performed at a rate of 20 °C min^{-1}, from 40 to 900 °C under nitrogen flow (70 ml min^{-1}), from 600 to 4000 cm^{-1} with a resolution of 4 cm^{-1}. To reduce the strong background absorption from water and carbon dioxide in the atmosphere, the optical bench was purged with nitrogen. In addition, a background spectrum was taken before

each analysis in order to zero the signal in the gas cell and to eliminate the contribution due to the amount of ambient water and carbon dioxide. The amount of sample in each TG-FTIR measurement varied between 6 and 8 mg. Data were collected using Agilent Resolution Pro version 5.2.0.

A PerkinElmer differential scanning calorimeter Pyris Diamond was used. Solid samples (8–10 mg) were crimped in aluminum pans and scanned from 30 to 550 °C at 10 °C min^{-1} under nitrogen flow and from 150 to 550 °C at 5 °C min^{-1} under airflow. A pinhole was made on the pan to allow the release of gases. Empty pans were used as references. The calorimeter was calibrated with indium as a standard.

The LIBS analysis was performed using the Modì double-pulse LIBS instrument in the "Smart" configuration, equipped with a dual-pulse laser (Nd-YAG, λ = 1064 nm, single-pulse energy up to 60 mJ in 10 ns) and a non-intensified double-grating spectrometer (AvaSpec Dual-Channel Fiber Optic Spectrometer from Avantes). The spectrometer simultaneously covers the spectral interval between 200 and 430 nm (with a resolution of 0.1 nm) and between 415 and 900 nm (with resolution of 0.3 nm). The inter-pulse delay was fixed at 1 μs, whereas the acquisition gate and delay were set at 2.48 ms and 2 μs, respectively. To analyze the samples, it was necessary to prepare a pellet that was at least 2–3 mm thick by applying a pressure of about 10 atm using a hydraulic press. Each LIBS spectrum corresponded to five laser shots in different sample points.

Raman spectra were recorded on a Raman Invia system (Renishaw) equipped with CCD detector with a resolution of 1800 lines/mm, coupled to an imaging microscope with 10×, 50× and 100× magnifications. The HeNe laser at 633 nm was used as an excitation source and was filtered to give a laser density power at the exit of the objective lens which varied from 0.1 to 2 W mm^{-2}. Several measurements were performed, adjusting the laser fluence to 0.5 W mm^{-2}, to ensure that the heating produced by the laser was minimized and the sample was not altered. Typically, a 50× magnification was used and the spot size diameter was about 2–3 μm. To register the Raman spectra, we took ten different points randomly from each pigment under the same conditions. Each spectrum was averaged over four scans corresponding to a collection time of 30 s.

A Nicolet 510 Fourier-transform infrared spectrometer equipped with a DTGS detector was used for transmittance measurements on KBr pellets. FTIR spectra were recorded with a resolution of 4 cm^{-1}, and 32 scans were taken in order to obtain an appropriate signal-to-noise ratio. The spectral range was measured between 4000 and 400 cm^{-1}.

A Siemens D-500 X-ray diffractometer with Bragg–Brentano optics was operated in $\theta/2\theta$ from 4° to 70° with a step scan of 0°, 2° using the CuKa radiation and a secondary graphite monochromator for the characterization of the powdered samples. Results were compared with the ICDD database in order to determine the phases present in the sample.

Results and discussion

FTIR spectra, FTIR signals and their attributions for the black samples investigated are reported in Fig. S.1 of ESI and Table 2.

Table 2

FTIR absorption peak table together with their attributions for the black samples investigated (bone blacks, vine blacks and lampblacks)

Sample	Absorption/cm^{-1}	Attribution	Species	References
Bone blacks (Kremer/Zecchi)	3450 (broad)	ν O–H	H_2O	[29] the correct refenence is [38] Vila et al
	1620 (broad)	δ O–H		
	1456, 872, 712	ν C–O $(CO_3)^{2-}$	Calcite hydroxyapatite ($Ca_5(PO_4)_3OH$)	[17] the correct refenence is [21]Van Loon A, Boon JJ.
	1090, 1030,	ν P–O $(PO_4)^{3-}$		[7] the correct refenence is [32] Tomasini et al.
	604	δ P–O $(PO_4)^{3-}$		
	2050	ν SCN^-	Proteinaceous residues	[29] the correct refenence is [38] Vila et al
	962	ν Si–O	Silicates	[46]the correct refenence is [54] Silverstein.
	872, 799	δ Si–O		

Sample	Absorption/cm^{-1}	Attribution	Species	References
Vine Black Zecchi	3450 (broad)	ν O–H	OH group of hydrated species and confined H_2O	[35] the correct reference is [32] Tomasini Siracusano
	1636	δ O–H	H_2O trapped	[29] the correct refenence is [38] Vila et al
	1030	ν Si–O/S–O $(SO_4)^{2-}$	Clays/sulfates	[29, 35] the correct refenence is [38] Vila et aland [32] Tomasini Siracusan
	520, 464	ν Fe–O	Iron oxides	[47] the correct reference is [55] spepi et al
Vine Black Kremer	3390 broad	ν O–H	OH group of hydrated species and confined H_2O	[29, 35] the correct refenence is [38] Vila et aland [32] Tomasini Siracusan
	3060	ν C–H aromatic	Aromatic residues	
	870–700 range	δ C–H aromatic		[35, 46] the correct referencies are32 and54
	1595, 1430	ν C–C aromatic		
	2980, 2920, 2850	ν C–H aliphatic	Aliphatic residues	[35, 46]the correct referencies are32 and54
	1300–1400 range	δ C–H aliphatic		
	1022	ν Si–O	Clays	[46]he correct refenence is [54] Silverstein.
	872, 800	ν Si–O		

Sample	Absorption/cm^{-1}	Attribution	Species	References
	520, 460	*v* Fe–O	Iron oxides	[47]he correct reference is [55] spepi et al

The LIBS and FTIR spectra of bone and ivory black pigments showed very similar spectral features. LIBS spectra presented a strong signal relative to the atomic emission of calcium at 393 and 397 nm (saturated signals) and a signal at 247.8 nm due to the atomic emission of carbon (Fig. S.2 of ESI). The main emission lines of Mg and Fe are also present. The FTIR spectra (Table 2 and Fig. S.1 of ESI) highlighted the signals due to water, carbonates and P–O bond vibration in agreement with the presence of calcite and hydroxyapatite ($Ca_5(PO_4)_3OH$), as expected for pigments obtained by bone calcination [32], as well as spectral features ascribable to SCN groups, deriving from collagen pyrolysis. Silicates are also detectable [28][32]. The XRD pattern confirmed the presence of hydroxyapatite and silicates, allowing the identification of quartz, feldspars and illite (Fig. S.3 of ESI). The data are coherent with the animal origin of the pigments, in agreement with the literature [28, 34][32, 38].

The LIBS spectra of the vine black pigments showed signals due to the atomic emissions of Mg (279.5, 280.2 and 285.1 nm) and Fe (371.9, 373.4, 373.7, 374.5 and 374.8 nm) (Fig. 1).

Fig. 1

LIBS spectra of vine black from Zecchi (black line) and Kremer (dotted line). I and II indicate neutral and single ionized species, respectively

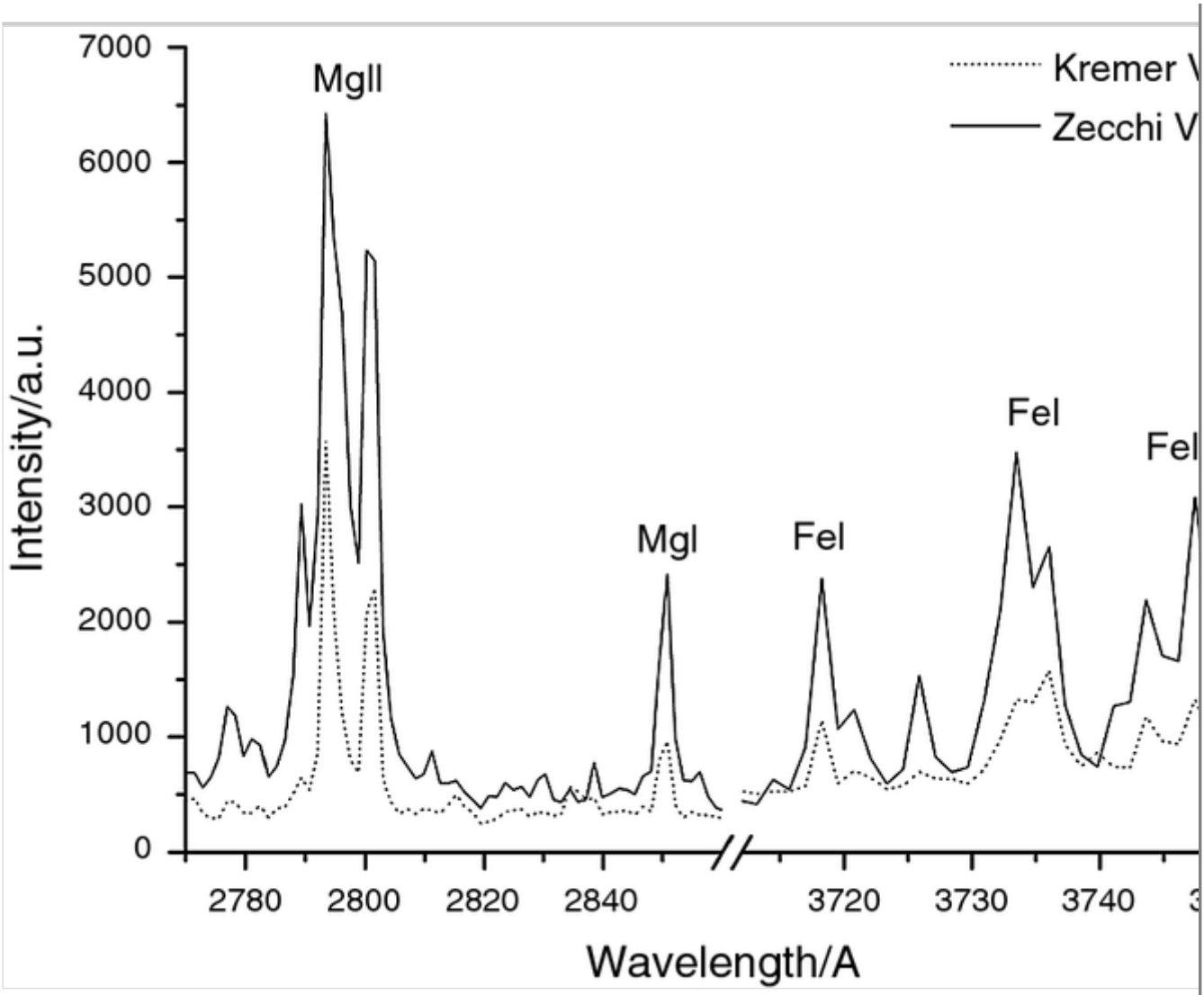

The FTIR spectrum of vine black from Zecchi showed the presence of silicates, in agreement with the literature [11]. XRD confirmed the presence of clays and other mineral phases, allowing the identification of talc ($Mg_3Si_4O_{10}(OH)_2$), tiptopite $K_2(Na,Ca)_2Li_3Be_6(PO_4)_6(OH)_2{\cdot}(H_2O)$, quartz ($SiO_2$), dolomite ($MgCa(CO_3)_2$) and kaolinite ($Al_4[(OH)_8Si_4O_{10}]$). Relatively low amounts of calcite ($CaCO_3$) and gypsum ($CaSO_4{\cdot}2H_2O$) were also detected by XRD (Fig. S.4 of ESI). The spectral features of vine black from Kremer presented signals ascribable to silicates and metal oxides, in agreement with Vila et al. [34][38]. Absorption peaks related to aromatic and aliphatic compounds were also clearly visible in the FTIR spectrum, in agreement with the presence of a non-crystalline material detected by XRD, in the form of a high background. XRD enabled the identification of relatively low amounts of quartz (SiO_2), dolomite ($MgCa(CO_3)_2$), kaolinite ($Al_4[(OH)_8Si_4O_{10}]$), calcite ($CaCO_3$) and gypsum ($CaSO_4{\cdot}2H_2O$).

Interestingly, these data are in disagreement with those reported by Tomasini et al. [28][32] who mainly highlighted the presence of barium sulfate in the vine black from Kremer. Barium sulfate is a filler commonly used in pigment

manufacturing, and its presence in commercial pigments might be inconsistent and unrelated to the pigment production.

The LIBS spectra of the lampblack pigments showed signals due to the atomic emission of carbon (247.8, 283.6, 392.0 and 426.7 nm). Lampblack from Kremer showed a small signal due to manganese at 257 nm (Fig. 2), whose presence could be due to small amounts of added manganese oxide, which has not been reported before for this pigment [11, 34, 1138]. The XRD pattern of both lampblacks does not show any crystallographic phase (Fig. S.5 of ESI), and the infrared spectra do not present significant spectral features, indicating that these pigments are mainly composed of amorphous charcoal.

Fig. 2

LIBS spectra of lampblack from Zecchi (black line) and Kremer (dotted line). I and II indicate neutral and single ionized species, respectively

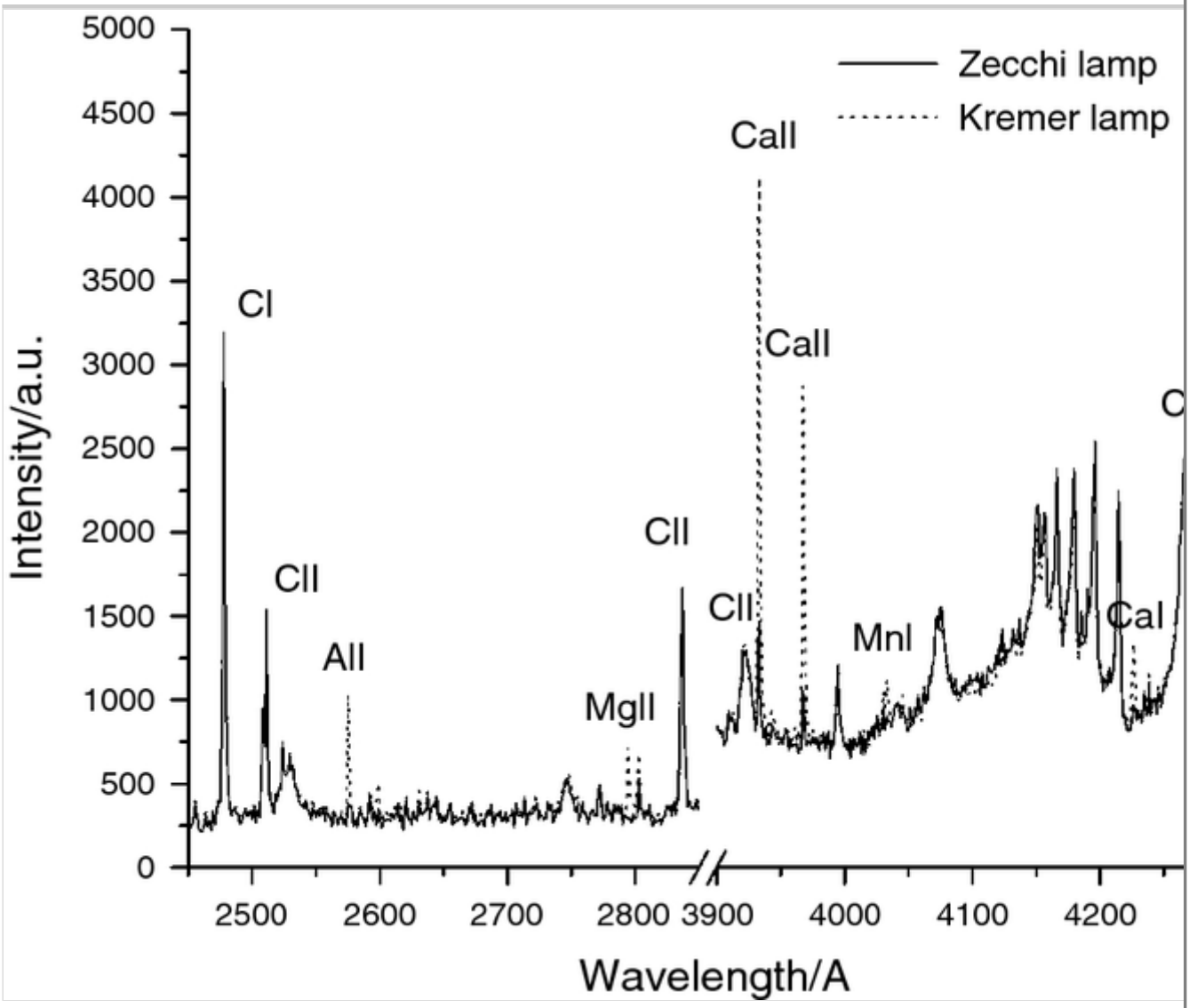

Raman has been extensively used for the identification of black pigments in the literature as it is the only technique which allows the direct detection of amorphous carbon [10, 11, 12, 13, 14, 15, 16, 17, 18, 19, 20, 21, 54, 55, 56, 57, 58][10, 12, 13, 14, 15, 16, 17, 18, 19, 56, 57, 58, 59, 60]. The Raman spectra in the range 500–1800 cm^{-1} of all samples analyzed are shown in Fig. 3.

Fig. 3

Raman spectra from 500 to 1800 cm^{-1} of all the black samples

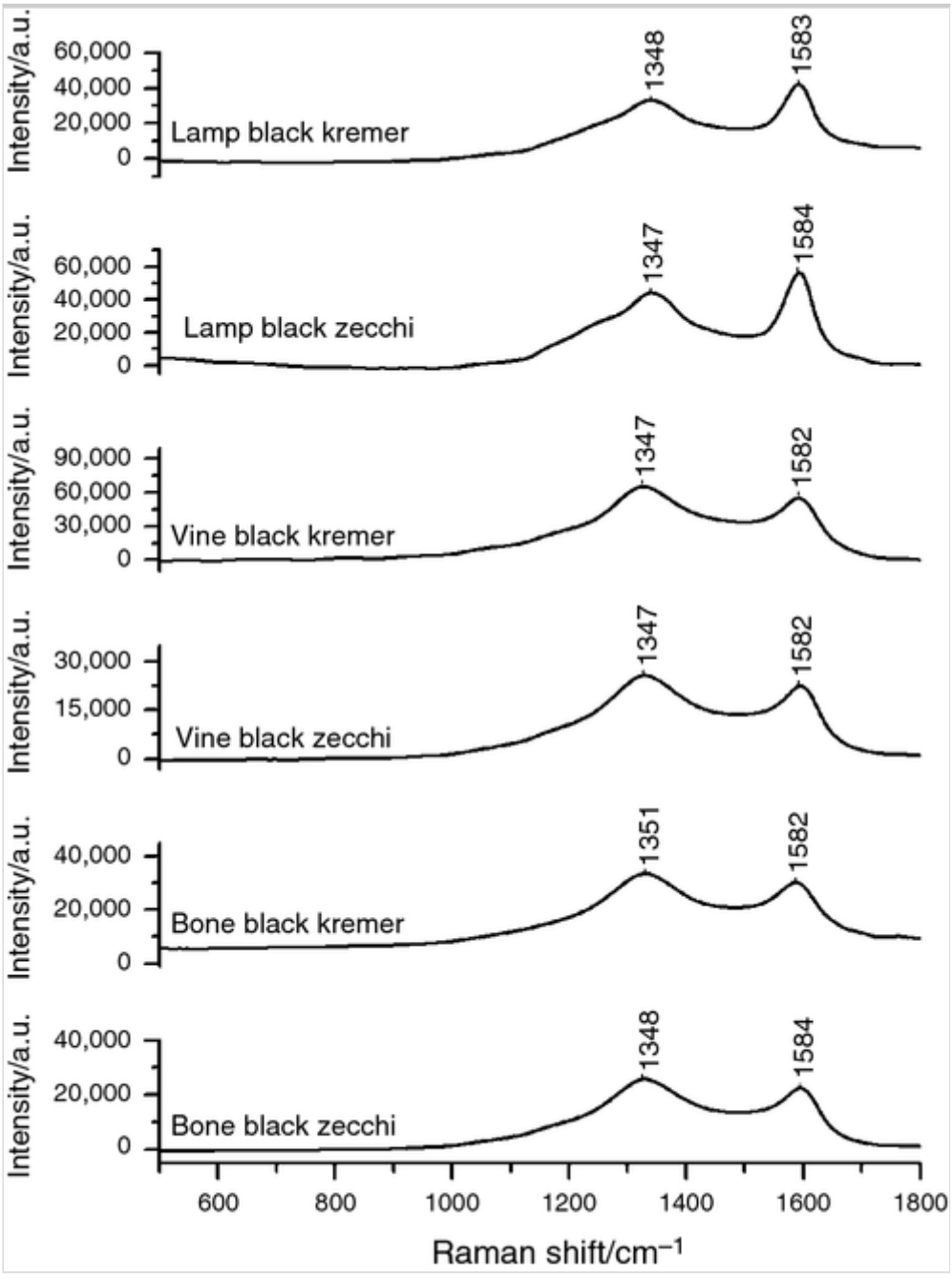

All the spectra obtained were very similar, showing a typical signal of a poorly organized microcrystalline graphite [12, 13, 14, 15, 16, 17, 18, 19], as observed in the literature for an array of black-based pigments [11].

The peak at about 1582 cm^{-1} is due to an “in-plane” displacement of the carbons strongly coupled in the hexagonal sheets and is called ***G*** (graphite) mode. This band is the only signal in a single perfect crystal graphite, thus corresponding to an ideal graphitic lattice vibration mode with E_{2g} symmetry [38][39].

When disorder is introduced into the graphite structure, this band broadens and an additional peak appears at about 1350 cm^{-1}, which is usually called the “disorder-induced” or ***D*** (disorder) mode, which corresponds to a graphitic lattice vibration mode with A_{1g} symmetry. Other weaker “disorder bands” appear in the Raman spectra, as the disorder of graphite increases. These bands are called ***D2*** (shoulder of ***G*** mode around 1620 cm^{-1}), ***D3*** (the strongest at around 1500 cm^{-1}) and ***D4*** (shoulder of ***D*** around 1150 cm^{-1}) [8][12].

In order to improve the accuracy in the determination of spectroscopic parameters such as peak position, bandwidth and intensity, a curve fitting was carried out for each spectrum [11, 12]. Several fits were tried leaving all the spectroscopic parameters free to progress. The best fitting was obtained for the six samples with four Gaussian bands (band D, D2, D3 and D4) and one Lorentzian band (band G) (see Fig. 4, as an example). The result of this fitting was in good agreement with recently published work [11, 12].

Fig. 4

Raman spectrum of lampblack Zecchi (black line) with the corresponding curve fitted bands (Gaussian dotted lines)

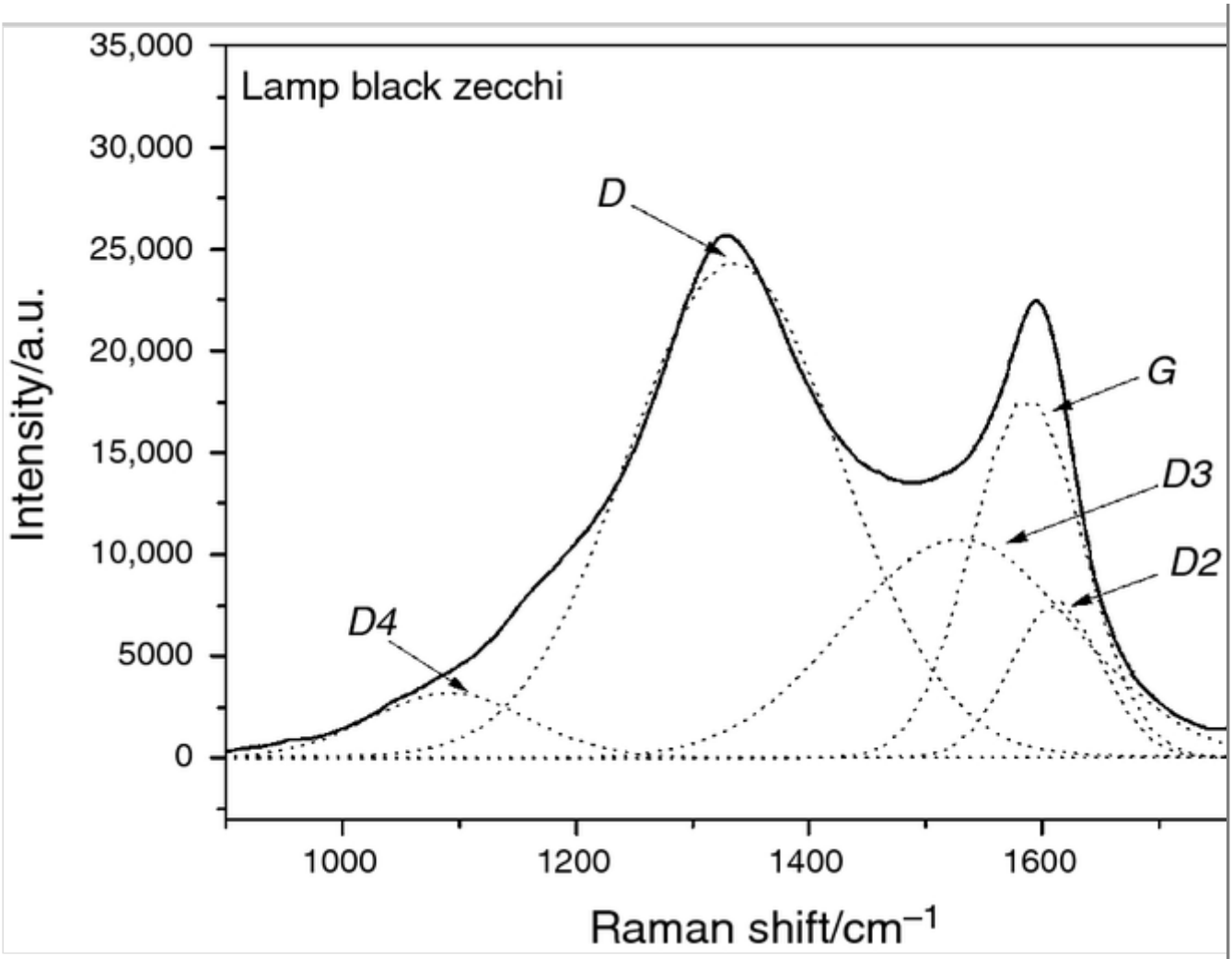

Table 3 summarizes all the Raman spectroscopic parameters obtained after curve fitting the experimental spectra using Gaussian and Lorentzian bands.

Table 3

Raman spectroscopic parameters obtained after curve fitting the experimental spectra (Lorentzian and Gaussian bands) of all the samples analyzed and the same values for pure microcrystalline graphite

Sample	**Peak position/cm^{-1}**	**Intensity (peak Area)**	R^2	L_a/nm
Microcrystalline graphite [24]				
G	1582	235		
D	1369	184		5.6
Bone black—Zecchi				
G	1592	86		
D	1352	432	0.73	0.9
D2	1602	69		
D3	1518	88		

Sample	Peak position/cm^{-1}	Intensity (peak Area)	R^2	L_a/nm
D4	1102	63		
Bone black—Kremer				
G	1593	102		
D	1349	458	0.72	0.9
D2	1603	71		
D3	1519	94		
D4	1104	73		
Vine black—Zecchi				
G	1590	83		
D	1354	434	0.75	0.8
D2	1601	59		
D3	1520	80		
D4	1096	57		
Vine black—Kremer				
G	1587	79		
D	1338	535	0.76	0.6
D2	1608	86		
D3	1522	77		
D4	1108	88		
Lampblack—Zecchi				
G	1590	184		
D	1346	546	0.68	1.5
D2	1600	67		
D3	1526	172		
D4	1095	69		
Lampblack—Kremer				
G	1592	168		
D	1358	494	0.67	1.5
D2	1601	74		
D3	1524	156		

Sample	Peak position/cm^{-1}	Intensity (peak Area)	R^2	L_a/nm
D4	1097	73		

All samples showed R^2 values (corresponding to the $D/(G + D+D2)$ area ratio) higher than 0.5, thus indicating the presence of amorphous material [5, 6, 8][10, 11, 12]. This was confirmed by the L_a values (L_a (nm) = 4.4 $[D/G]^{-1}$) in the range of 0.6–1.5. As demonstrated by Tuinstra and Koenig [59], these values indicate a low degree of structural order, which is very high in vine and bone blacks (0.6–0.9) and lower in lampblack (1.5), which show a small graphitic domain in addition to an amorphous phase [10, 12, 60][10, 12, 62].

The spectra of vine black show additional bands at 224, 243 and 290 cm^{-1} due to symmetric bending of the Fe–O bond, bands at 408, 495, 608 and 659 cm^{-1} due to symmetric and asymmetric vibrational modes of Fe–O bond [61] and bands at 196 and 172 cm^{-1} due to stretching of Mg–O bond [62] (Fig. S.6 of ESI).

All the pigments were characterized by TG-FTIR and DSC under inert (nitrogen) atmosphere (Figs. 5–8) and by TG and DSC under oxidative atmosphere (Figs. 9–10).

Fig. 5

Thermogravimetric curve (left axis) and its DTG (right axis) under nitrogen flow at 10 °C min^{-1} heating rate of bone black (**a**), vine black (**b**) and lampblack (**c**) purchased from Zecchi and Kremer

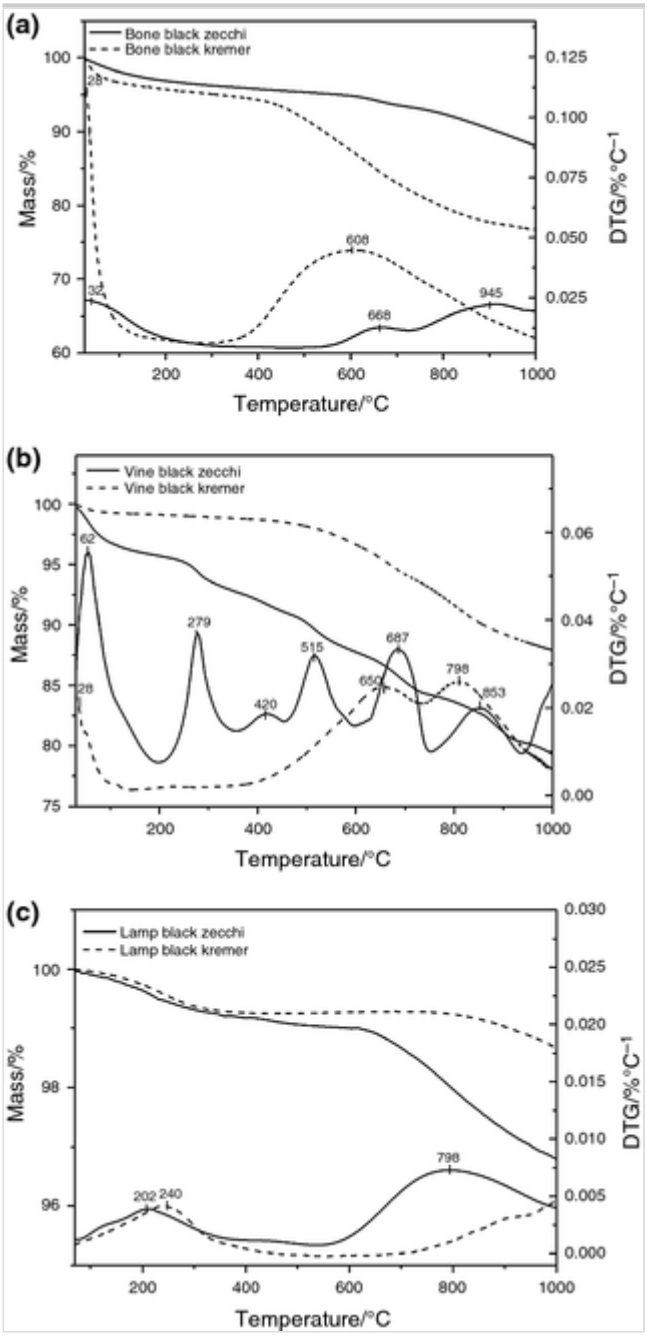

Figure 5 shows a comparison between the thermodegradative curves and the corresponding derivative curves recorded under nitrogen flow for each of the black pigments. Table 4 summarizes the experimental temperatures and the percentage weight losses of each thermal decomposition step.

Table 4

Temperatures (maximum of DTG curve), mass loss percentage of the thermal degradation steps and residual masses at 1000 °C of the black pigments studied under nitrogen flow

Step	Bone black		Vine black		Lampblack	
	Kremer	Zecchi	Kremer	Zecchi	Kremer	Zecchi

Step	Bone black		Vine black		Lampblack	
	Kremer	Zecchi	Kremer	Zecchi	Kremer	Zecchi
1	28 °C (4.7%)	30 °C (3.7%)	28.1 °C (1.3%)	63 °C (4.5%)		
2				279 °C (3.2%)	240 °C (1.3%)	202 °C (1.0%)
3				420 °C (1.8%)		
4				515 °C (3.3%)		
5	608°C[a] (18.4%)	600–900°C[b] (8.3%)	450–1000°C[c] (8.8%)	687 °C (3.6%)		
6						798°C[d] (2.3%)
7				853 °C (3.2%)		
Residual mass at 1000 °C	76.9%	88%	89.9%	80.4%	98.7%	96.7%
[a]Maximum of derivative in the range 400–1000 °C						
[b]Total mass loss in the range 600–1000 °C						
[c]Total mass loss in the range 450–1000 °C						
[d]Maximum of derivative in the range 600–1000 °C						

Bone and vine black pigments present mass losses below 100 °C in the TG curves (DTG peaks between 40 and 70 °C, Fig. 5a–c), corresponding to broad endothermic peaks centered between 74 °C and 90 °C (Fig. S.7–S.9 of ESI) of the DSC. These are due to the loss of moisture, in accordance with the relative FTIR spectra of the evolved gases, presenting a series of narrow bands typical of moisture water (4000–3500 cm^{-1} and 2000–1300 cm^{-1}, Figs. 6, 8).

Fig. 6

FTIR spectra of evolved gas from the decomposition of bone black (Zecchi) under nitrogen atmosphere: (**a**) degradation at 668 °C, (**b**) degradation at 945 °C

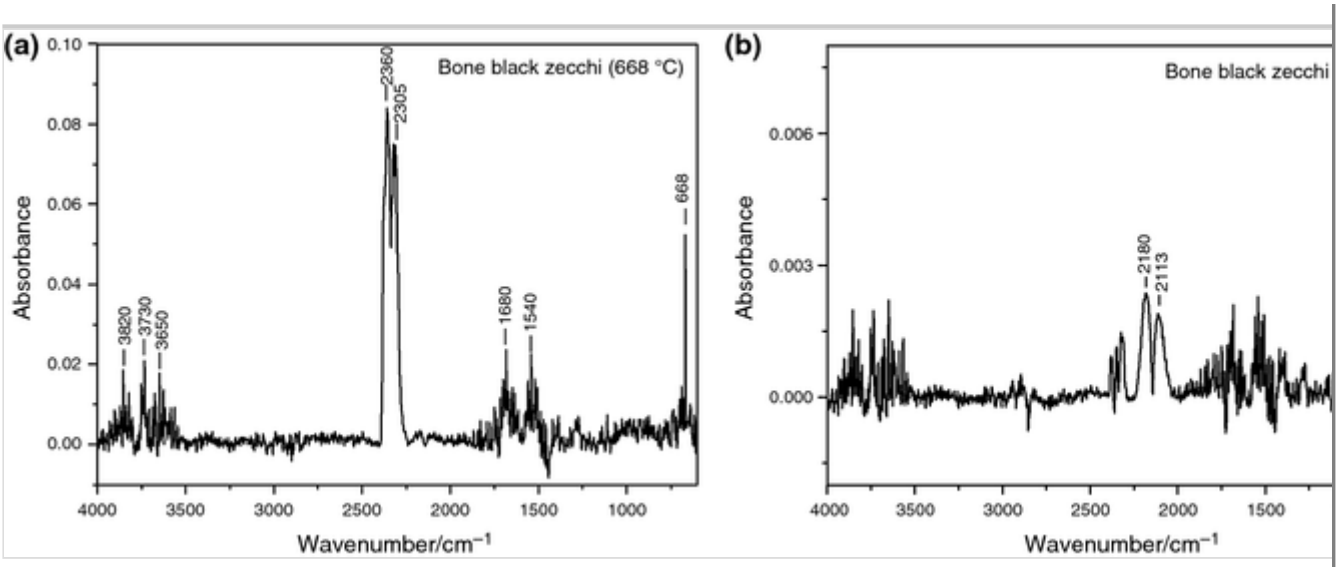

The thermogravimetric curves of bone black (Fig. 5a) exhibited a second mass loss with the DTG peak centered at 600–700 °C. As shown by the FTIR spectra of the evolved gases, this mass loss is mainly due to the CO_2 release (2360, 2305 cm^{-1} and 668 cm^{-1}) (Fig. 6a), likely due to the decomposition of residues of bone calcite. The sample from Zecchi shows a third mass loss above 900 °C. The FTIR spectra show a weak absorption due to CO traces (two broad bands at 2180 and 2113 cm^{-1}) (Fig. 6b). The formation of CO at these temperatures could be the result of traces of iron oxides, not detected by LIBS, or, possibly other trace minerals, which can catalyze the formation of CO from carbon. [54][64].

The thermogravimetric curves of vine black from Zecchi were quite different from those of the Kremer pigment (Fig. 5b) and show that the former is a more complex mixture of different materials. Except for the first DTG peak due to water release (DSC endothermic peak under 90 °C), all the mass losses in the 200–1000 °C temperature range of the Zecchi Vine Black are due to CO_2 elimination, as evident from the TG-FTIR analysis (Fig. S.10 in ESI). The mass loss around 280 °C corresponds to an endothermic process, such as decarboxylation (DSC peak centered at 288 °C, Fig. 7). This may be due to the decomposition of residual pyrolysis products originating from vine cellulose and lignin [53]. The mass loss centered at 515 °C, which is well visible for the Zecchi sample, may be due to the presence of hydrated silicates included in vine black during the combustion of wood, in accordance with the crystalline phases identified by XRD. The thermal decomposition of crystalline silicates, sulfates and carbonates identified by XRD in vine black from Kremer is not observed, as their mass losses are most likely hidden by the broad mass loss in the range 450–900 °C [53].

Fig. 7

DSC curve of Zecchi vine black in nitrogen atmosphere at 20 °C min^{-1}

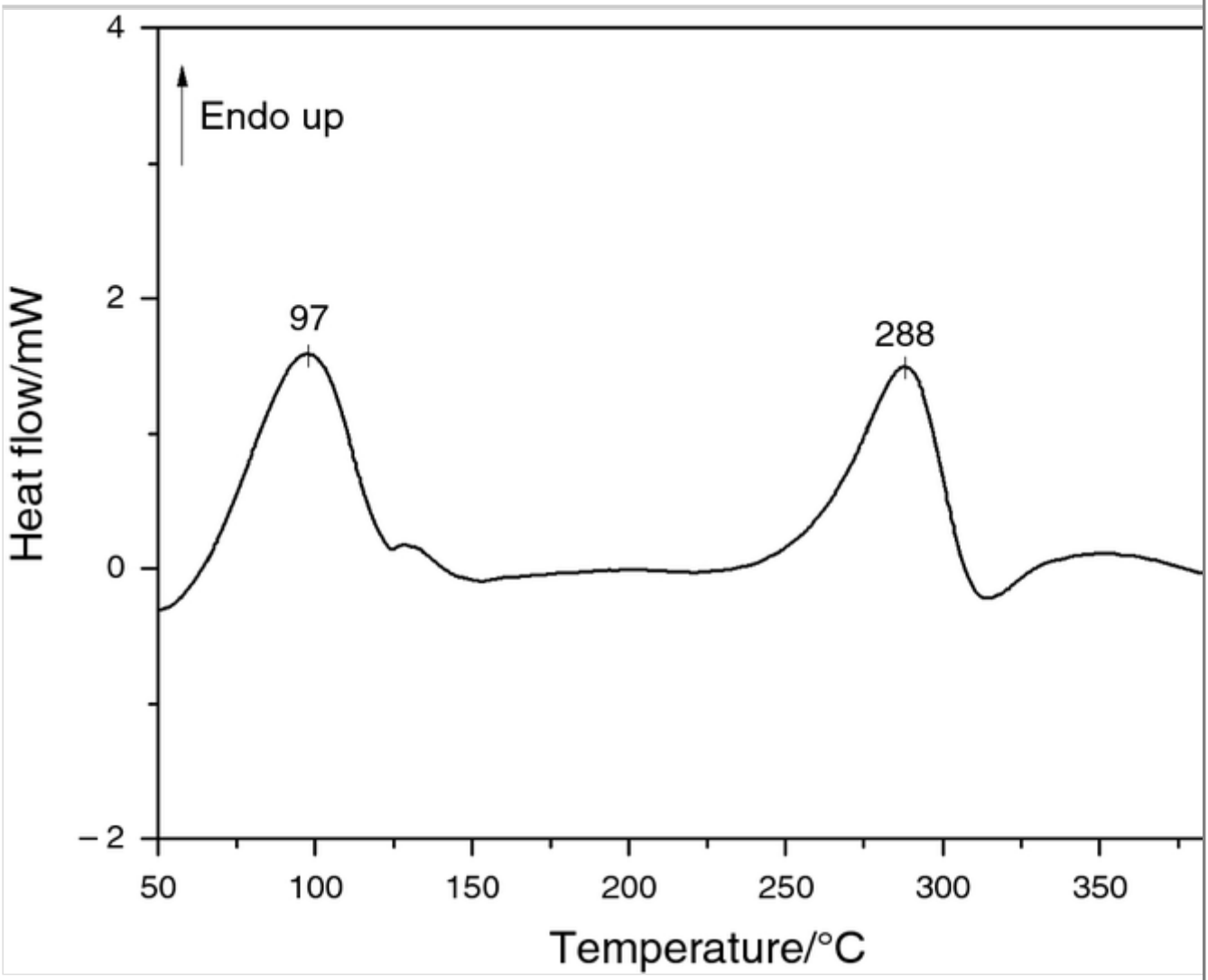

The FTIR spectra of gases evolved from the pyrolytic decomposition of the Kremer sample at 650 °C (Fig. 8) show the spectral features of CO_2 as well as those of CH_4 (3010 and 1303 cm^{-1}). At about 800 °C, CO_2 and CO are released in addition to signals ascribable to organic species (signals from 1300 to 1754 cm^{-1} due to C–C, C–O stretching and C–H bending, and signals in the range 2860–2950 cm^{-1} due to C–H stretching). Methane, ethane, methanol, carbon dioxide and monoxide are in fact typical products of the pyrolysis of lignin and cellulose (from residues of vine plants during the production of this pigment) formed over 600 °C [63][65]. The presence of organic residues in the vine black from Kremer was also suggested by the FTIR spectra and XRD pattern of this sample, showing characteristic vibrations of aromatic rings and non-crystalline material, respectively. The production process of vine black purchased from Zecchi is very likely to be different from that purchased from Kremer, based on the absence of pyrolysis products of lignin and cellulose, as indicated by all techniques investigated. This suggests that vine black purchased from Zecchi was produced at a higher temperature, or with prolonged heating with respect to that purchased from Kremer.

Fig. 8

FTIR spectra of evolved gas from decomposition of vine black from Kremer under nitrogen atmosphere at 650 °C

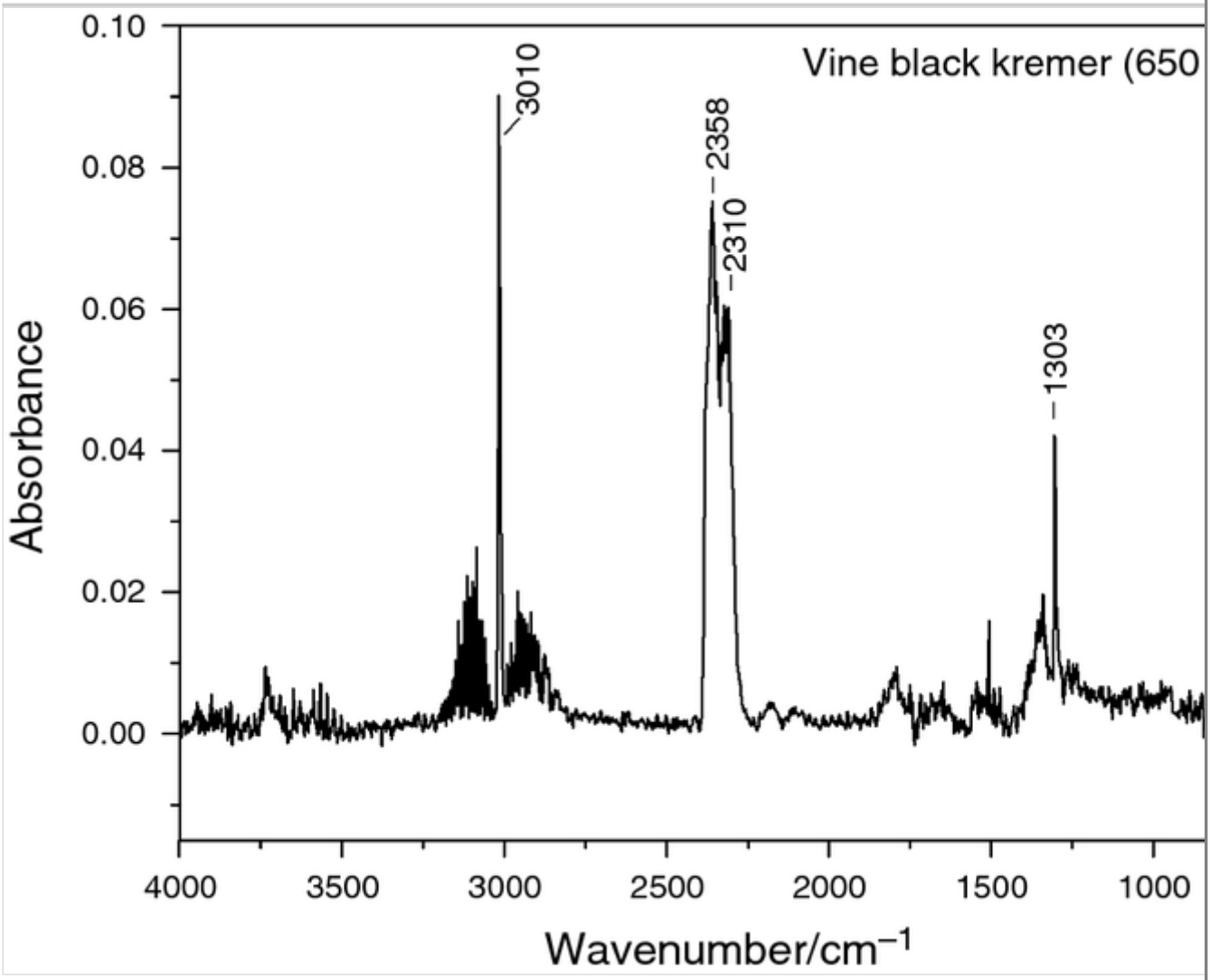

The lampblacks show the simplest thermal profiles with the highest residual mass (Fig. 5c). The DSC curves do not show any peaks in the temperature range 50–550 °C (Fig. S.11 of ESI), and the TG-FTIR analysis of the gaseous species evolved from the thermal decomposition of lampblack did not reveal the formation of any species.

All these features suggest that the lampblack samples were the purest samples, with the highest percentage of carbon.

Figure 9 compares the thermo-oxidative degradation curves and the corresponding derivative curves recorded under airflow for each of the black pigments. Table 5 summarizes the experimental temperatures and the percentage weight losses of the thermal decomposition steps.

Fig. 9

Thermogravimetric curve (left axis) and its DTG (right axis) under nitrogen flow at 10 °C min^{-1} heating rate of bone black (**a**), vine black (**b**) and lampblack (**c**) from Zecchi and Kremer

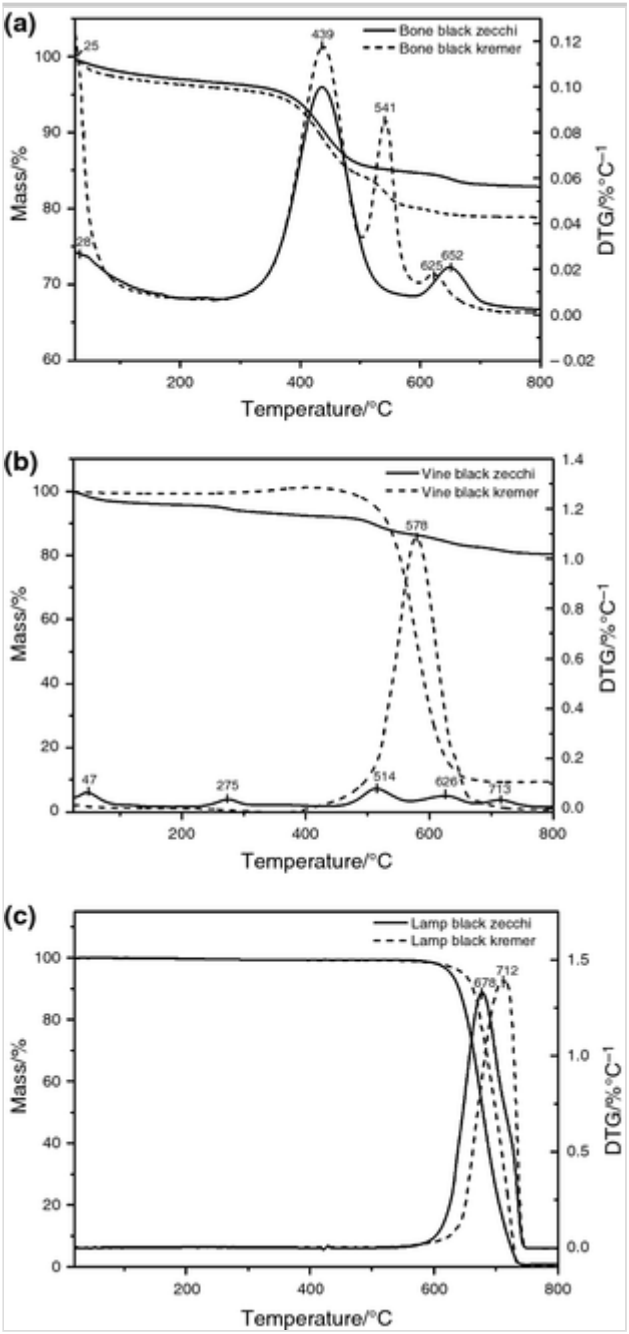

Table 5

Temperatures (maximum of the DTG curve), mass loss percentage of the thermal degradation steps and residual masses at 800 °C of black pigments under airflow

Step	Bone black		Vine black		Lampblack	
	Kremer	Zecchi	Kremer	Zecchi	Kremer	Zecchi
[a]Total mass loss in the range 300–550 °C						
[b]Total mass loss in the range 400–700 °C						

Step	Bone black		Vine black		Lampblack	
	Kremer	Zecchi	Kremer	Zecchi	Kremer	Zecchi
1	25 °C (3.7%)	28 °C (3.1%)		47 °C (4.1%)		
2				275 °C (2.9%)		
3	439 °C (12.1%)	439°C[a] (11.8)				
4	541 °C (4.2%)		578°C[b] (90.5%)	514 °C (6.1%)		
5	625 °C (1.1%)	652 °C (2.2%)		626 °C (3.7%)		
6				713 °C (2.7%)	712 °C (99.2%)	678 °C (99.3%)
Residual mass at 800 °C	78.9%	82.9%	9.5%	80.5%	0.8%	0.7%
[a]Total mass loss in the range 300–550 °C						
[b]Total mass loss in the range 400–700 °C						

Mass losses occurring below 50 °C (DTG peaks between 25 °C, 28 °C and 47 °C, Fig. 9a, b) are due to the loss of moisture, which is absent in the lampblack samples. Measurements performed in air confirmed that bone and vine blacks purchased from Zecchi and Kremer had a different composition and thermal profile. The DSC curves relative to these samples show a strong exothermic peak in the range 420–530 °C (Fig. 10), which may be ascribed to the combustion of charcoal as well as organic residues from proteinaceous material at lower (439 °C) and higher (541 °C) molecular weights for the bone blacks, and wood (578 °C) for the vine blacks. The sum of the areas of the DSC exothermic peaks of the bone black from Kremer is almost the same than that of the single exothermic peak of the bone black from Zecchi, thus confirming that the samples contain almost the same quantity of organic material as demonstrated by the very similar values of the residual masses at 800 °C.

Fig. 10

DSC curve in air atmosphere at 20 °C min^{-1} of Bone Black (**a**) and Vine Black samples (**b**) purchased from Zecchi and Kremer

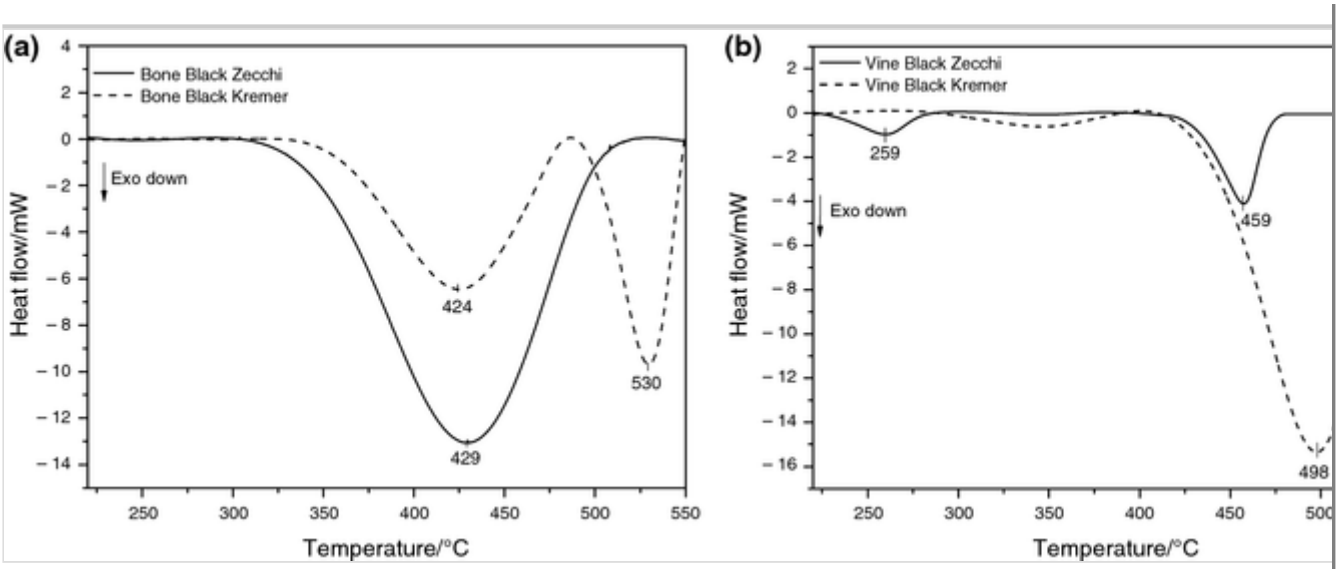

The vine black purchased from Kremer appears to comprise the highest content of carbonaceous material (about 90%) with respect to that purchased from Zecchi, showing a single broad mass loss in the range 300–550 °C, corresponding to a strong exothermic peak at 498 °C in the DSC (with an area about 10 times higher than that of the corresponding exothermic peak of vine black from Zecchi Fig. 10b). The mass loss observed above 600 °C in the bone blacks (652 and 625 °C for Zecchi and Kremer, respectively) is due to the degradation of the residual calcium carbonate originating from the bones, as identified with other techniques.

The combustion of lampblack samples occurs at higher temperatures than the other samples (678 and 712 °C for Zecchi and Kremer, respectively). This might relate to the different sizes of carbon particles in each sample [53].

Results obtained are summarized in Table 6 and Table S.1 where spectroscopic and thermogravimetric data were combined to describe the qualitative and semiquantitative composition of the different pigments.

Table 6

Summary of main, secondary and traces constituents of carbon black samples studied

Black pigment	Main constituent (above 75%)	Secondary constituents (below 20%)	Traces (below 5%)
Bone—Zecchi	Hydroxyapatite ($Ca_5(PO_4)_3OH$) Calcium carbonate ($CaCO_3$)	Amorphous carbon (charcoal) Organic species originating from the pyrolysis of collagen	Water

Black pigment	Main constituent (above 75%)	Secondary constituents (below 20%)	Traces (below 5%)
Bone—Kremer	Hydroxyapatite ($Ca_5(PO_4)_3OH$) Calcium carbonate ($CaCO_3$)	Amorphous carbon (charcoal) Organic species originating from the pyrolysis of collagen	Water
Vine—Zecchi	Ashes Iron oxides (Fe_xO_y) Magnesium oxide (MgO)	Amorphous carbon (charcoal) Organic species originating from the pyrolysis of lignin and cellulose (aliphatic)	Water Silicates Calcium carbonate ($CaCO_3$)
Vine—Kremer	Amorphous carbon (charcoal) Organic species originating from the pyrolysis of lignin and cellulose (aliphatic/aromatic)		Water Iron oxides (Fe_xO_y) Magnesium oxide (MgO) Calcium carbonate ($CaCO_3$)
Lamp—Zecchi	Amorphous carbon with small graphitic domains		
Lamp—Kremer	Amorphous carbon with small graphitic domains		Manganese dioxide (MnO_2)

AQ4

Conclusions

The multi-analytical approach applied enabled us to identify the different constituents (both organic and inorganic) of the pigments and their relative contents, highlighting qualitative and—for the first time—quantitative differences, based on the type of pigment (bone, vine and lamp) and the manufacturer (Zecchi and Kremer):

- In the two bone blacks, $CaCO_3$ and $Ca_5(PO_4)_3OH$, ascribable to the pyrolysis of bones, were found as main constituents, and organic material, in particular amorphous carbon and nitrogen-containing materials originating from the pyrolysis of collagen, as secondary constituents.

- In the two vine blacks, organic material residues were identified, originating from the pyrolysis of vine cellulose and lignin, as well as amorphous carbon. However, the results highlighted a key difference between the Kremer and Zecchi products: The first is in fact made up of 90% organic material, while the second presents only 10%. Inorganic compounds

(sulfates, carbonates, clays and phosphates) had been added to the pigment as fillers, to produce pigments with suitable artistic properties. [28]

- The two lampblacks were essentially made up of amorphous carbon. The lampblack purchased from Kremer also contained a small percentage of MnO_2. The manganese oxide is blackish in color, suggesting that it was added to the pigment formulation, most likely to increase its covering power.

The present paper, complementing previous studies reported in the literature, has established the complete qualitative and quantitative characterization of the composition and of the thermal (oxidative) degradation patterns of different synthetic black pigments based on carbon, whose use has been established since prehistoric times. Data provide key information for the pigment identification in samples of unknown composition, as well as potentially important information for model studies on the physicochemical behavior of paints under natural and accelerated aging, aimed at understanding degradation patterns and planning efficient conservation strategies of paintings and polychromies for the future generations.

Publisher's Note

Springer Nature remains neutral with regard to jurisdictional claims in published maps and institutional affiliations.

Acknowledgements

This work was supported by the projects *CMOP Cleaning Modern Oil Paints*—founded by JPI Cultural Heritage Call “Heritage + ; Transnational collaborative research project” and *Advanced analytical pyrolysis to study polymers in renewable energy, environment, cultural heritage*—founded by the University of Pisa, PRA_2018_26.

Electronic supplementary material

Below is the link to the electronic supplementary material.

Supplementary material 1 (DOCX 1462 kb)

References

1. Sandu ICA, Bracci S, Sandu I, Lobefaro M. Integrated analytical study for the authentication of five Russian icons (XVI–XVII centuries). Microsc Res Tech. 2009;72:755–65.

2. Lluveras-Tenorio A, Parlanti F, Degano I, Lorenzetti G, Demosthenous D, Colombini MP, Rasmussen KL. Spectroscopic and mass spectrometric approach to define the Cyprus Orthodox icon tradition—The first known occurrence of Indian lac in Greece/Europe. Microchem J. 2017;131:112–9.

3. Colombo L. I colori degli antichi, Ed. Nardini, 1995.
AQ5

4. Feller RL. Artist's pigments: a handbook of their history and characteristics, Ed. C.U.P.aN.G.o. Art. Vol. 1, 1986.

5. Mayer R. The artist's handbook of materials and techniques, New York, 1970.

6. Roldán C, Villaverde V, Ródenas I, Novelli F, Murcia S. Preliminary analysis of Palaeolithic black pigments in plaquettes from the Parpallócave (Gandía, Spain) carried out by means of non-destructive techniques. J Archaeol Sci. 2013;40:744–54.

7. Rampazzi L, Campo L, Cariati F, Tanda G, Colombini MP. Prehistoric wall paintings: the case of the Domus de Janas necropolis (Sardinia, Italy). Archaeometry. 2007;49(3):559–69.

8. Rasmussen KL, Lluveras-Tenorio A, Bonaduce I, Colombini MP, Birolo L, Galano E, Amoresano A, Doudna G, Bond AD, Palleschi V, Lorenzetti G, Legnaioli S, van der Plicht J, Gunneweg J. The constituents of the ink from a Qumran inkwell: new prospects for provenancing the ink on the Dead Sea Scrolls. J Archaeol Sci. 2012;39:2956–68.

9. Winters J, West Fitzhugh E. Artist's pigments: a handbook of their history and characterization (Ed BH Berrie). Oxford: Oxford University Press; 2007.

10. Jawhari T, Roid A, Casado J. Raman spectroscopic characterization of some commercially available carbon black materials. Carbon. 1995;33:1561–5.

11. Tomasini EP, Hala EB, Reinoso M, Di Liscia EJ, Maier MS. Micro-Raman spectroscopy of carbon-based black pigments. J Raman Spectrosc.

2012;43(11):1671–5.

12. Sadezky A, Muckenhber H, Grothe HR, Niesser R, Poschl R. Raman microscopy of soot and related carbonaceous materials: spectral analysis and structural information. Carbon. 2005;43:1731–42.

13. Van der Weerd J, Smith GD, Firth S, Clark RJK. Identification of black pigments on prehistoric Southwest American potsherds by infrared and Raman microscopy. J Archaeol Sci. 2004;311:429–1437.

14. Gayo MD. Pigmentos y colorants presentes en los bienes culturales, toma de muestras y metodes de analisis. Tecnica de diagnostico aplicadas a a la conservacion de los bienes muebles. Sevilla: IAPH Sevilla; 1986.

15. Creagh DC. The characterization of artefacts of cultural heritage significance using physical techniques. Radiat Phys Chem. 2005;74:426–42.

16. Perez-Rodriguez JL, Maqueda C, Jimenez de Haro MC, Rodriguez-Rubio P. Comparison between micro-Raman and micro-FTIR spectroscopy techniques for the characterization of pigments from Southern Spain Cultural Heritage. Atmos Environ. 1998;32:993–8.

17. Jimenez de Haro MC, Justo A, Duran A, Siguenza MB, Perez-Rodriguez JL, Bueno J. Air pollution and cultural heritage (ED. Jimenez CS). London: Blakerma Publisher; 2005.

18. Calamitou M, Siganidou M, Filippakis SE. X-ray analysis of pigments from Pella, Greece. Stud Conserv. 1983;28:117–21.

19. Beyssac O, Goffè B, Petitet JP, Froigneux E, Moreau M, Rouzaud JN. On the characterization of disordered and heterogeneous carbonaceous materials by Raman spectroscopy. Spectrochim Acta A. 2003;59:2267–76.

20. Parras-Guijarro D, Montejo-Gamez M, Ramos-Martos N, Sanchez A. Analysis of pigments and coverings by X-ray diffraction (XRD) and micro Raman spectroscopy (MRS) in the cemetery of Tutugi (Galera, Granada, Spain) and the settlement convento 2 (Montemayor, Córdoba, Spain). Spectrochim Acta A. 2006;64:1133–41.

21. Van Loon A, Boon JJ. Characterization of the deterioration of bone black in the 17th century Oranjezaal paintings using electron-microscopic and

micro-spectroscopic imaging techniques. Spectrochim Acta B. 1996;59:1601–9.

22. Anglos D, Couris S, Fotakis C. Laser induced breakdown spectroscopy in pigment identification. Appl Spectrosc. 1997;51:1025–31.

23. Anglos D, Balas S, Fotakis C. Laser spectroscopic and optical imaging techniques in chemical and structural diagnostics of painted artwork. Am Lab. 1999;31:60–7.

24. Corsi M, Palleschi V, Salvetti A, Tognoni E. Making LIBS quantitative: a critical review of the current approaches to the problem. Res Adv Appl Spectrosc. 2000;1:41–7.

25. Stratoudaki T, Xenakis D, Zafiropulos V, Anglos D. LIBS in the analysis of pigments in painted artworks. A database of pigments and spectra. In: Proceedings of the 5th international conference on optics within the life science, Berlin: Springer; 2000. p. 163–8.

26. Ciucci A, Corsi M, Palleschi V, Rastelli V, Salvetti A, Tognoni E. New procedure for quantitative elemental analysis by laser-induced plasma spectroscopy. Appl Spectrosc. 1999;53:960–4.

27. Burgio L, Clark RJH, Stratoudaki T, Doulgeredis M, Anglos D. Pigment identification. A dual analytical approach employing Laser Induced Breakdown Spectroscopy (LIBS) and Raman Microscopy. Appl Spectrosc. 2000;54:463–9.

28. Castillejo M, Martin M, Silva D, Stratoudaki T, Anglos D, Burgio L. Analysis of pigments in polychromes by use of Laser Induced Breakdown Spectroscopy and Raman microscopy. J Mol Struct. 2000;550:191–8.

29. Burgio L, Melessanaki K, Doulgeridis M, Clark RJH, Anglos D. Pigment identification in paintings employing laser induced breakdown spectroscopy and Raman microscopy. Spectrochim Acta B. 2001;56:905–13.

30. Smith DC, Bouchard M, Lorblanchet M. An initial Raman microscopic investigation of prehistoric rock art in caves of the Quercy District, SW France. J Raman Spectrosc. 1999;30:347–54.

31. Olin JS. The use of infrared spectrophotometry in the examination of paintings and ancient artifacts. Instrum News. 1996;17:4–5 Li D, Sun G. Coloration of textiles with self-dispersible carbon black nanoparticles. Dyes Pigments. 2007;72:144–9.

32. Tomasini E, Siracusano G, Maier MS. Spectroscopic, morphological and chemical characterization of historic pigments based on carbon. Paths for the identification of an artistic pigment. Microchem J. 2012;102:28–37.

33. Van't Hul-Ehrnreich EH. Infrared microspectroscopy for the analysis of old painting materials. Stud Conserv. 1970;15:175–82.

34. Carbò D, Reig B, Adelantado G, Martinez P. Fourier transform infrared spectroscopy and the analytical study of works of art for purposes of diagnosis and conservation. Anal Chim Acta. 1996;330:207–15.

35. Li D, Sun G. Coloration of textiles with self-dispersible carbon black nanoparticles. Dyes Pigments. 2007;72:144-149.

36. Duce C, Della Porta V, Tiné MR, Spepi A, Ghezzi L, Colombini MP. FTIR study of ageing of fast drying oil colour (FDOC) alkyd paint replicas. Spectrochim Acta A. 2014;130:214–21.

37. Pellegrini D, Duce C, Bonaduce I, Biagi S, Ghezzi L, Colombini MP. Fourier transform infrared spectroscopic study of rabbit glue/inorganic pigments mixtures in fresh and aged reference paint reconstructions. Microchem J. 2015;124:31–5.

38. Vila A, Ferrer N, García JF. Chemical composition of contemporary black printing inks based on infrared spectroscopy: basic information for the characterization and discrimination of artistic prints. Anal Chim Acta. 2007;591:97–105.

39. Edwards HGM, Chalmers JM. Raman Spectroscopy in archaeology and art history. Cambridge: Royal Society of Chemistry ED Cambridge; 2005.

40. Tascon M, Mastrangelo N, Gheco L, Gastaldi M, Quesada M, Marte F. Micro-spectroscopic analysis of pigments and carbonization layers on prehispanic rock art at the Oyola's caves, Argentina, using a stratigraphic approach. Microchem J. 2016;129:297–304.

41. Burgio L, Clark RJK. Library of FT-Raman spectra of pigments, minerals, pigment media and varnishes, and supplement to existing library of Raman spectra of pigments with visible excitation. Spectrochim Acta A. 2001;57:1491–503.

42. Duce C, Bramanti E, Ghezzi L, Bernazzani L, Bonaduce I, Colombini MP, Tinè MR. Interactions between inorganic pigments and proteinaceous binders in reference paint reconstructions. Dalton Trans. 2013;42:5775–986.

43. Duce C, Bernazzani L, Bramanti E, Spepi A, Colombini MP, Tinè MR. Alkyd artists' paints: do pigments affect the stability of the resin? A TG and DSC study on fast-drying oil colours. Pol Degrad Stab. 2014;105:48–58.

AQ6

44. Ghezzi L, Duce C, Bernazzani L, Bramanti E, Colombini MP, Tinè MR, Bonaduce I. Interactions between inorganic pigments and rabbit skin glue in reference paint reconstructions. J Therm Anal Calorim. 2015;122:315–22.

45. Bonaduce I, Carlyle L, Colombini MP, Duce C, Ferrari C, Ribechini E. New insights into the ageing of linseed oil paint binder: a qualitative and

quantitative analytical study. PLoS ONE. 2012;7:e49333. https://doi.org/10.1371/journal.pone.0049333.

46. Stacey RJ, Dyer J, Mussell C, Lluveras-Tenorio A, Colombini MP, Duce C, LaNasa J, Cantisani E, Prati S, Sciutto G, Mazzeo R, Sotiropoulou S, Rosi F, Miliani C, Cartechini L, Mazurek J, Schilling M. Ancient Encaustic: an experimental exploration of technology, ageing behaviour and approaches to analytical investigation. Microchem J. 2018;138:472–87.

47. La Nasa J, Di Marco F, Bernazzani L, Duce C, Spepi A, Ubaldi V, Degano I, Orsini S, Legnaioli S, Tiné MR, De Luca D, Modugno F. Aquazol as binder for retouching paints. An evaluation through analytical pyrolysis and thermal analysis. Polym Degrad Stab. 2017;144:508–19.

48. Tamburini D, Sardi D, Spepi A, Duce C, Tiné MR, Colombini MP, Bonaduce I. An investigation into the curing of urushi and tung oil films by thermoanalytical and mass spectrometric techniques. Polym Degrad Stab. 2016;134:251–64.

49. Tiné MR, Duce C. Calorimetric and thermo analytical techniques in cultural heritage. In: Lazzara G, Fakhrullin R, editors. Nanotechnologies and nano materials for diagnostic, conservation and restoration of cultural heritage. Amsterdam: Elsevier; 2018. p. 79–109. ISBN 978-0-12-813910-3.

50. Dohnalová Ž, Šulcová P, Bělina P, Vlček M, Gorodylova N. Brown pigments based on perovskite structure of $BiFeO_{3-\delta}$. J Therm Anal Calorim. 2018;133:421–8.

51. Dohnalova Z, Šulcova P, Bělina P. Pink NIR pigment based on Cr-doped $SrSnO_3$ preparation and characterization. J Therm Anal Calorim. https://doi.org/10.1007/s10973-019-08522-z

AQ7

52. Milia A, Bruno M, Cavallaro G, Lazzara G, Milioto S. Adsorption isotherms and thermal behavior of hybrids based on quercetin and inorganic fillers. J Therm Anal Calorim. https://doi.org/10.1007/s10973-019-08257-x

53. Gatta T, Campanella L, Coluzza C, Mambro V, Postorino P, Tomassetti M. Characterization of black pigments used in 30 BC fresco wall paint using instrumental methods and chemometry. Chem Cent J. 2012;6:S2–10.

54. Silverstein RM, Webster FX, Kiemle DJ. Spectrometric identification of organic compounds. 7th ed. New York: Wiley; 2005.

55. Spepi A, Duce C, Ferrari C, Gonzalez-Rivera J, Zaglicic Z, Domenici V, Pineider F, Tinè MR. A simple and versatile solvothermal configuration to synthesize superparamagnetic iron oxide nanoparticles using a coaxial Microwave antenna. RSC Adv. 2016;6:104366–74.

56. Nakamizo N, Kammereck R, Walker PL Jr. Laser Raman studies on carbons. Carbon. 1974;12:259–67.

57. Mernagh TP, Cooney RP, Johnson RA. Raman spectra of graphon carbon black. Carbon. 1984;22:39–42.

58. Cuesta A, Dhamelincourt P, Laureyns J, Martinez-Alonso A, Tascòn JMD. Raman microprobe studies on carbon materials. Carbon. 1994;32:1523–32.

59. Nikiel L, Jagodzinski PW. Raman spectroscopic characterization of graphites: a reevaluation of spectra/structure correlation. Carbon. 1991;31:1313–7.

60. Pawlyta M, Rouzaud JN, Duber S. Raman microspectroscopy characterization of carbon blacks: spectral analysis and structural information. Carbon. 2015;84:479–90.

61. Tuinstra F, Koenig JL. Raman spectrum of graphite. J Chem Phys. 1970;53:1126–33.

62. Ebner E, Burow D, Panke J, Borger A, Feldhoff A, Atanassova P, Valenciano J, Work M, Ruhl E. Carbon blacks for lead-acid batteries in micro-hybrid applications—studied by transmission electron microscopy and Raman spectroscopy. J Power Sour. 2013;222:554–60.

63. Farrow RL, Benner RE, Nagelberg AS, Mattern PL. Characterization of surface oxides by Raman spectroscopy. Thin Solid Films. 1980;73:353–8.

64. Dolci S, Domenici V, Duce V, Tinè MR, Ierardi V, Valbusa U. Ultrasmall superparamagnetic iron oxide nanoparticles with titanium-N,N-dialkylcarbamato coating. Mater Res Express. 2014;1:35401–10.

AQ8

65. Rath J, Staudinger G. Cracking reaction of tar from pyrolysis of spruce wood. Fuel. 2001;80:1379–89.